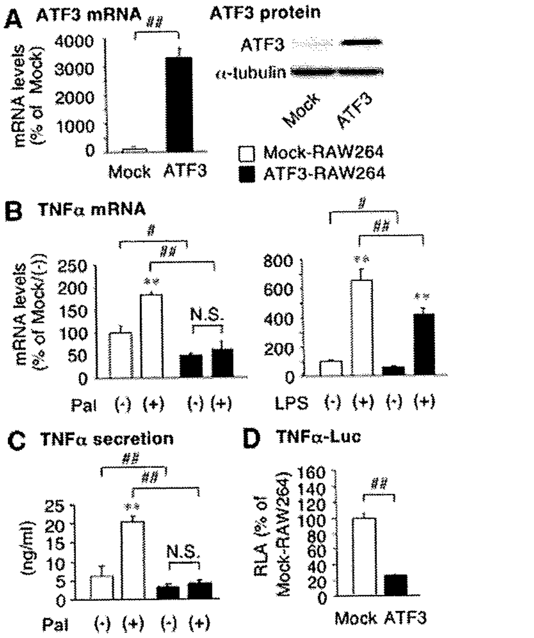

Figure 4. Effect of ATF3 overexpression on saturated fatty acid–induced TNFα production in cultured macrophages. A, Retrovirus-mediated stable overexpression of a full-length mouse ATF3 cDNA in RAW264 macrophages (ATF3-RAW264) and control RAW264 macrophages (Mock-RAW264). Effect of ATF3 overexpression on the palmitate- and LPS-induced TNFα mRNA expression (B) and secretion (C). D, Effect of ATF3 overexpression on the TNFα promoter activity. Pal indicates palmitate 200 μmol/L; LPS, LPS 10 ng/mL. **$P<0.01$ vs the respective control; #$P<0.05$, ##$P<0.01$ (n=4).

mRNA expression was significantly reduced relative to control RAW264 macrophages (Mock-RAW264) ($P<0.01$) (Figure 4B). We confirmed that the palmitate- and LPS-induced increase in TNFα secretion in the ATF3-RAW264 culture media is significantly reduced relative to Mock-RAW264 ($P<0.01$) (Figure 4C). We also observed with a luciferase reporter assay that TNFα promoter activity is markedly inhibited in ATF3-RAW264 relative to Mock-RAW264 (Figure 4D). Similarly, the palmitate-induced increase in IL-6 and inducible nitric oxide synthase was significantly reduced in ATF3-RAW264 relative to Mock-RAW264 (Online Figure III, a). These observations indicate that overexpression of ATF3 is capable of reducing the saturated fatty acid–induced proinflammatory cytokine production in macrophages.

We next examined the effect of knockdown of endogenous ATF3 gene expression in RAW264 macrophages. Stable knockdown of ATF3 using 2 independent short hairpin loop RNAs (shATF3#1 and shATF3#3) was confirmed by Western blotting (Figure 5A). The ATF3–knocked-down RAW264 macrophages (shATF3#1-RAW264 and shATF3#3-RAW264) exhibited significant enhancement of the palmitate-induced TNFα mRNA expression relative to control RAW264 macrophages (shGFP-RAW264) ($P<0.01$) (Figure 5B). The effect of ATF3 knockdown on TNFα mRNA expression persisted until 24 hours after stimulation with LPS (Figure 5C). Knockdown of ATF3 also significantly increased TNFα secretion in the culture media ($P<0.01$) (Figure 5D). Furthermore, we observed that the TNFα promoter activity is

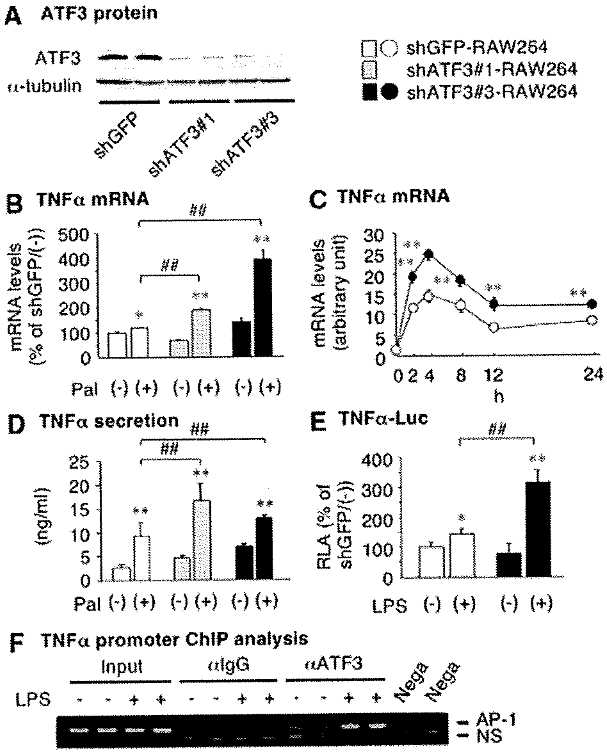

Figure 5. Effect of ATF3 knockdown on saturated fatty acid–induced TNFα production in cultured macrophages. A, Retrovirus-mediated ATF3 knockdown in RAW264 macrophages. Two short hairpin loop RNAs (shATF3#1 and shATF3#3) designed to target different sequences within ATF3 mRNA effectively knocked down endogenous ATF3 in RAW264 macrophages. B, Effect of ATF3 knockdown on the palmitate-induced TNFα mRNA expression. C, Time course of the LPS-induced TNFα mRNA expression in RAW264 macrophages. D, Effect of ATF3 knockdown on the palmitate-induced TNFα secretion. E, Effect of ATF3 knockdown on the TNFα promoter activity. shATF3#1-RAW264 and shATF3#3-RAW264 indicate ATF3–knocked-down RAW264 macrophages; shGFP-RAW264, control RAW264 macrophages; Pal, palmitate 200 μmol/L; LPS, LPS 10 ng/mL. **$P<0.01$ vs the respective control; #$P<0.05$, ##$P<0.01$ (n=4). F, TNFα promoter chromatin immunoprecipitation analysis with chromatin extracts prepared from RAW264 macrophages treated with or without LPS (100 ng/mL) for 6 hours. αATF3 indicates anti-ATF3 antibody; αIgG, normal rabbit IgG; Nega, negative control without template; NS, nonspecific band.

significantly increased in shATF3#3-RAW264 relative to shGFP-RAW264 ($P<0.01$) (Figure 5E). These observations suggest that once induced by the saturated fatty acids/TLR4 signaling, ATF3 attenuates the saturated fatty acid–induced TNFα production in macrophages, thereby constitute a negative feedback mechanism to reduce the TLR4 signaling induction of proinflammatory cytokine production. This notion is consistent with a recent report by Gilchrist et al that ATF3 acts as a negative regulator of the LPS-induced TLR4 signaling.[25]

In the proximal region of the IL-6 and IL-12b promoters, ATF3-binding ATF/CREB sites are located close to NF-κB binding sites.[25] NF-κB and ATF3, both of which are activated by saturated fatty acids/TLR4 signaling, can positively and negatively regulate their target proinflammatory cytokines, respectively.[25] However, there are no consensus sequences corresponding to the ATF/CREB site close to the NF-κB–binding site (−534 bp) in the proximal region of TNFα promoter. In this study, we performed chromatin immunoprecipitation analysis with RAW264 macrophages and found that ATF3 is recruited to the region containing the activator protein (AP)-1 site (−926 bp) of the endogenous TNFα promoter (Figure 5F). This observation is consistent with a previous report that ATF3 binds to the AP-1 site.[26] It is, therefore, interesting to know how ATF3 negatively regulates TNFα and IL-6 production via its distinct binding sites; the AP-1 and ATF/CREB sites, respectively. In addition, histone deacetylase and heat shock transcription factor 1 are required for the action of ATF3 on the IL-6 promoter.[25,27] It is, therefore, important to identify ATF3-interacting proteins on the TNFα promoter.

Distinct Intracellular Signaling Pathways Plays a Role in the Palmitate- and LPS-Induced ATF3 Expression

In this study, we demonstrated that saturated fatty acids induce ATF3 expression in macrophages through the TLR4/NF-κB pathway, which is consistent with the previous report on LPS.[25] Besides NF-κB, mitogen-activated protein kinases (MAPKs) are an important intracellular signaling pathway downstream of TLR4,[28] and c-Jun N-terminal kinase (JNK) and p38 MAPK have been reported to play a role in ATF3 expression in certain cell types.[29,30] We, therefore, examined the involvement of MAPKs in the saturated fatty acid– and LPS-induced ATF3 mRNA expression and found that SB20358038, a p38 MAPK inhibitor, inhibits significantly the palmitate-induced ATF3 mRNA expression ($P<0.01$) (Online Figure IV). On the other hand, SP600125, a JNK inhibitor, inhibited most effectively the LPS-induced ATF3 mRNA expression ($P<0.01$) (Online Figure IV). Moreover, we found that ERK plays a major role in the palmitate-induced TNFα mRNA expression, whereas other MAPKs may also contribute to the LPS-induced TNFα mRNA expression (Online Figure IV). These observations, taken together, suggest that distinct intracellular signaling pathways may mediate the saturated fatty acid– and LPS-induced ATF3 mRNA expression through TLR4. It is interesting to know how endogenous and exogenous TLR4 ligands such as saturated fatty acids, oxidized phospholipids, and cytosolic and nuclear proteins, and LPS,[12,28,31] exert their effects through the unique signaling pathways, thereby leading to a variety of cellular responses.

Transgenic Overexpression of ATF3 Attenuates Macrophage Activation in Obese Adipose Tissue

To elucidate the role of ATF3 in macrophages infiltrated into obese adipose tissue, we developed transgenic mice overexpressing human ATF3 in macrophages under the control of SR-A promoter (ATF3 Tg) (Online Figure V, a).[32] Genomic Southern blot analysis identified 9 (line 2), 13 (line 25), and 20 (line 35) transgene copies in independent founder lines (data not shown). Western blot analysis of ATF3 revealed 3-fold and 2-fold increase in ATF3 protein levels in bone marrow–derived macrophages from lines 25 and 35, respectively, relative to wild-type mice (Online Figure V, b). In this

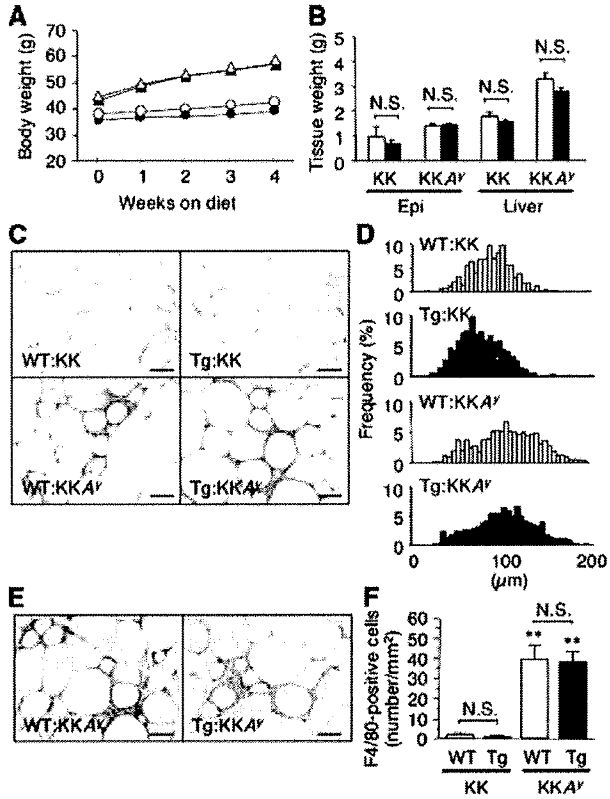

Figure 6. Adipocyte hypertrophy and macrophage infiltration in the adipose tissue from transgenic mice with macrophage-specific ATF3 overexpression. A, Time course of body weight. ○, WT:KK; ●, transgenic (Tg):KK; △, WT:KKA^y; ▲, Tg:KKA^y. B, The epididymal adipose tissue (Epi) and liver weights. Open bar, WT; closed bar, Tg. C, Hematoxylin/eosin staining of the epididymal adipose tissue. D, Histogram of diameters of adipocytes in the epididymal adipose tissue. E, F4/80 immunostaining of the epididymal adipose tissue. F, Cell count of F4/80-positive cells in the epididymal adipose tissue. **$P<0.01$ vs the respective KK background (n=6 to 13).

study, there was no significant increase in ATF3 levels in line 2 macrophages (Online Figure V, b). We observed essentially the same data using peritoneal macrophages from 3 independent transgenic lines (Online Figure V, b).

We crossed ATF3 Tg (line 35) with genetically obese KKA^y mice and obtained 4 genotypes as the F1 generation (wild-type on the KK background [WT:KK], ATF3 Tg on the KK background [ATF3 Tg:KK], wild-type on the KKA^y background [WT:KKA^y], and ATF3 Tg on the KKA^y background [ATF3 Tg:KKA^y]) at a Mendelian ratio (data not shown). In this study, WT:KK and ATF3 Tg:KK were fed standard diet and WT:KKA^y and ATF3 Tg:KKA^y were fed high-fat diet for 4 weeks. During the course of high-fat diet feeding, transgenic overexpression of ATF3 in macrophages did not affect significantly body weight and epididymal fat weight on KK and KKA^y backgrounds (Figure 6A and 6B). The liver weight tended to be decreased in ATF3 Tg:KKA^y relative to WT:KKA^y, but the difference did not reach statistical significance (Figure 6B). Histological analysis showed no apparent difference in adipocyte cell size between genotypes (Figure 6C and 6D). There was no significant difference in obesity-induced macrophage infiltration be-

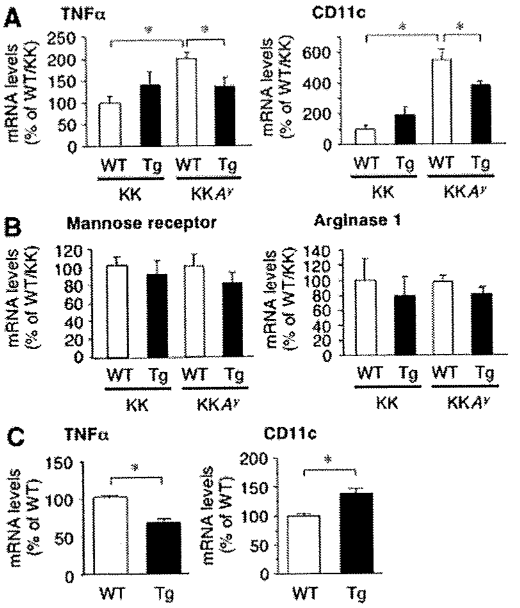

Figure 7. Effect of ATF3 on activation and polarization of adipose tissue macrophages and peritoneal macrophages from macrophage-specific ATF3 transgenic mice. A and B, mRNA expression of M1 markers (TNFα and CD11c) (A) and M2 markers (mannose receptor and arginase 1) (B) in the epididymal adipose tissue from WT:KK, Tg:KK, WT:KKA^y, and Tg:KKA^y mice. C, mRNA expression of M1 markers (TNFα and CD11c) in peritoneal macrophages from WT and Tg on the C57BL/6J background. *$P<0.05$ (n=6 to 13).

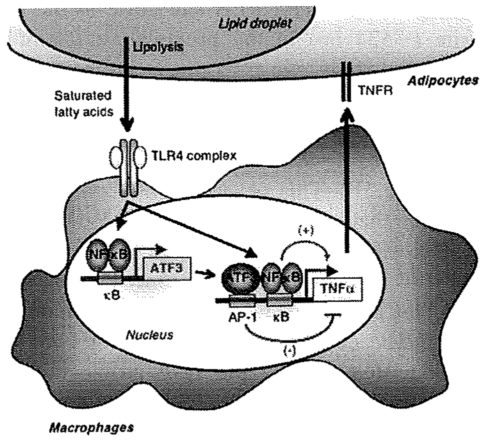

Figure 8. Negative feedback mechanism involving ATF3 as a transcriptional repressor of saturated fatty acid/TLR4 signaling in macrophages in obese adipose tissue. In the interaction between adipocytes and macrophages, ATF3 is upregulated in macrophages through the saturated fatty acids/TLR4/NF-κB signaling. Once induced, ATF3 can transcriptionally reduce the saturated fatty acids/TLR4 signaling–induced proinflammatory cytokine production. Our data have identified ATF3 as a transcriptional repressor of saturated fatty acid/TLR4 signaling, thereby revealing the negative feedback mechanism that attenuates macrophage activation in obese adipose tissue. TNFR indicates TNFα receptor; AP-1 and κB, AP-1– and NF-κB–binding elements, respectively.

tween WT:KKA^y and ATF3 Tg:KKA^y (Figure 6E and 6F). These observations suggest that transgenic overexpression of ATF3 in macrophages does not affect adipocyte hypertrophy and macrophage infiltration in obese adipose tissue.

We also examined the effect of ATF3 on macrophage activation and polarization in the adipose tissue from transgenic mice with macrophage-specific overexpression of ATF3. We observed a marked increase in TNFα mRNA expression in the adipose tissue from WT:KKA^y relative to WT:KK, which was significantly attenuated in ATF3 Tg:KKA^y ($P<0.05$) (Figure 7A). In this study, M1 macrophage marker CD11c was also increased in the adipose tissue from WT:KKA^y relative to WT:KK (Figure 7B), which was effectively inhibited in ATF3 Tg:KKA^y ($P<0.05$) (Figure 7A). Moreover, IL-6 mRNA expression tended to be decreased in the adipose tissue from ATF3 Tg:KKA^y mice relative to WT:KKA^y (Online Figure III, b). By contrast, we found no significant difference in mRNA expression of M2 macrophage markers, mannose receptor and arginase 1, among genotypes (Figure 7B). These observations suggest that overexpression of ATF3 in macrophages is capable of inhibiting macrophage activation and M1 polarization in the adipose tissue in vivo (Figure 8).

We next examined TNFα and CD11c mRNA expression in peritoneal macrophages prepared from ATF3 Tg and WT on the C57BL/6J background. Similar to the data on the adipose tissue (Figure 7A), TNFα mRNA expression was significantly suppressed in peritoneal macrophages from ATF3 Tg relative to WT ($P<0.05$) (Figure 7C). Interestingly, CD11c mRNA expression in peritoneal macrophages was rather higher in ATF3 Tg than in WT ($P<0.05$) (Figure 7C). In this regard, using ATF3-RAW264 and shATF3-RAW264, we did not observe that ATF3 has impact on CD11c mRNA expression in vitro (data not shown), suggesting that CD11c may not be a transcriptional target of ATF3 in macrophages. Further studies are needed to elucidate the role of ATF3 in obesity-induced M1 polarization of adipose tissue macrophages. Global ATF3-deficient mice are viable,[19,25] but the role of ATF3 in glucose/lipid metabolism has not been elucidated. Because activation and polarization of adipose tissue macrophages play an important role in the metabolic status,[7–9] studies with ATF3 Tg and macrophage-specific ATF3-deficient mice would help elucidate the pathophysiologic role of ATF3 in macrophages in adipose tissue inflammation and systemic glucose/lipid metabolism.

In conclusion, ATF3 is upregulated in macrophages in the interaction between adipocytes and macrophages through the saturated fatty acids/TLR4/NF-κB signaling. Once induced, ATF3 can transcriptionally reduce the saturated fatty acids/TLR4 signaling induction of proinflammatory cytokine production. Among known negative regulators of TLR4 signaling,[28] ATF3 is unique in that it represses the TLR4 target genes via a transcriptional mechanism. This study provides evidence that ATF3 acts as a transcriptional repressor of saturated fatty acids/TLR4 signaling, thereby revealing the negative feedback mechanism that attenuates macrophage activation in obese adipose tissue (Figure 8). Our data also suggest that activation of ATF3 in macrophages may offer a novel therapeutic strategy to prevent or treat obesity-induced adipose tissue inflammation.

Acknowledgments

We thank Ai Togo for secretarial assistance and Takanori Kunieda and Tae Mieda for technical assistance. We are also grateful to the members of the Ogawa laboratory for discussions.

Sources of Funding

This work was supported in part by a Grant-in-Aid for Scientific Research from the Ministry of Education, Culture, Sports, Science and Technology of Japan and Ministry of Health, Labor and Welfare of Japan and research grants from Takeda Science Foundation and Takeda Medical Research Foundation.

Disclosures

None.

References

1. Grundy SM, Brewer HB, Jr, Cleeman JI, Smith SC Jr, Lenfant C. Definition of metabolic syndrome: report of the National Heart, Lung, and Blood Institute/American Heart Association conference on scientific issues related to definition. *Circulation*. 2004;109:433–438.
2. Hotamisligil GS. Inflammation and metabolic disorders. *Nature*. 2006; 444:860–867.
3. Berg AH, Scherer PE. Adipose tissue, inflammation, and cardiovascular disease. *Circ Res*. 2005;96:939–949.
4. Matsuzawa Y, Funahashi T, Nakamura T. Molecular mechanism of metabolic syndrome X: contribution of adipocytokines adipocyte-derived bioactive substances. *Ann N Y Acad Sci*. 1999;892:146–154.
5. Weisberg SP, McCann D, Desai M, Rosenbaum M, Leibel RL, Ferrante AW Jr. Obesity is associated with macrophage accumulation in adipose tissue. *J Clin Invest*. 2003;112:1796–1808.
6. Suganami T, Nishida J, Ogawa Y. A paracrine loop between adipocytes and macrophages aggravates inflammatory changes: role of free fatty acids and tumor necrosis factor α. *Arterioscler Thromb Vasc Biol*. 2005; 25:2062–2068.
7. Lumeng CN, Bodzin JL, Saltiel AR. Obesity induces a phenotypic switch in adipose tissue macrophage polarization. *J Clin Invest*. 2007;117: 175–184.
8. Kang K, Reilly SM, Karabacak V, Gangl MR, Fitzgerald K, Hatano B, Lee CH. Adipocyte-derived Th2 cytokines and myeloid PPARδ regulate macrophage polarization and insulin sensitivity. *Cell Metab*. 2008;7: 485–495.
9. Odegaard JI, Ricardo-Gonzalez RR, Red Eagle A, Vats D, Morel CR, Goforth MH, Subramanian V, Mukundan L, Ferrante AW, Chawla A. Alternative M2 activation of Kupffer cells by PPARδ ameliorates obesity-induced insulin resistance. *Cell Metab*. 2008;7:496–507.
10. Cao H, Gerhold K, Mayers JR, Wiest MM, Watkins SM, Hotamisligil GS. Identification of a lipokine, a lipid hormone linking adipose tissue to systemic metabolism. *Cell*. 2008;134:933–944.
11. Unger RH. Lipotoxicity in the pathogenesis of obesity-dependent NIDDM. Genetic and clinical implications. *Diabetes*. 1995;44:863–870.
12. Suganami T, Tanimoto-Koyama K, Nishida J, Itoh M, Yuan X, Mizuarai S, Kotani H, Yamaoka S, Miyake K, Aoe S, Kamei Y, Ogawa Y. Role of the Toll-like receptor 4/NF-κB pathway in saturated fatty acid-induced inflammatory changes in the interaction between adipocytes and macrophages. *Arterioscler Thromb Vasc Biol*. 2007;27:84–91.
13. Lee JY, Sohn KH, Rhee SH, Hwang D. Saturated fatty acids, but not unsaturated fatty acids, induce the expression of cyclooxygenase-2 mediated through Toll-like receptor 4. *J Biol Chem*. 2001;276: 16683–16689.
14. Shi H, Kokoeva MV, Inouye K, Tzameli I, Yin H, Flier JS. TLR4 links innate immunity and fatty acid-induced insulin resistance. *J Clin Invest*. 2006;116:3015–3025.
15. Suganami T, Mieda T, Itoh M, Shimoda Y, Kamei Y, Ogawa Y. Attenuation of obesity-induced adipose tissue inflammation in C3H/HeJ mice carrying a Toll-like receptor 4 mutation. *Biochem Biophys Res Commun*. 2007;354:45–49.
16. Poggi M, Bastelica D, Gual P, Iglesias MA, Gremeaux T, Knauf C, Peiretti F, Verdier M, Juhan-Vague I, Tanti JF, Burcelin R, Alessi MC. C3H/HeJ mice carrying a Toll-like receptor 4 mutation are protected against the development of insulin resistance in white adipose tissue in response to a high-fat diet. *Diabetologia*. 2007;50:1267–1276.
17. Tsukumo DM, Carvalho-Filho MA, Carvalheira JB, Prada PO, Hirabara SM, Schenka AA, Araujo EP, Vassallo J, Curi R, Velloso LA, Saad MJ. Loss-of-function mutation in Toll-like receptor 4 prevents diet-induced obesity and insulin resistance. *Diabetes*. 2007;56:1986–1998.
18. Cai Y, Zhang C, Nawa T, Aso T, Tanaka M, Oshiro S, Ichijo H, Kitajima S. Homocysteine-responsive ATF3 gene expression in human vascular endothelial cells: activation of c-Jun NH_2-terminal kinase and promoter response element. *Blood*. 2000;96:2140–2148.
19. Hartman MG, Lu D, Kim ML, Kociba GJ, Shukri T, Buteau J, Wang X, Frankel WL, Guttridge D, Prentki M, Grey ST, Ron D, Hai T. Role for activating transcription factor 3 in stress-induced beta-cell apoptosis. *Mol Cell Biol*. 2004;24:5721–5732.
20. Poltorak A, He X, Smirnova I, Liu MY, Van Huffel C, Du X, Birdwell D, Alejos E, Silva M, Galanos C, Freudenberg M, Ricciardi-Castagnoli P, Layton B, Beutler B. Defective LPS signaling in C3H/HeJ and C57BL/10ScCr mice: mutations in TLR4 gene. *Science*. 1998;282:2085–2088.
21. Kitagawa K, Wada T, Furuichi K, Hashimoto H, Ishiwata Y, Asano M, Takeya M, Kuziel WA, Matsushima K, Mukaida N, Yokoyama H. Blockade of CCR2 ameliorates progressive fibrosis in kidney. *Am J Pathol*. 2004;165:237–246.
22. Tamura K, Hua B, Adachi S, Guney I, Kawauchi J, Morioka M, Tamamori-Adachi M, Tanaka Y, Nakabeppu Y, Sunamori M, Sedivy JM, Kitajima S. Stress response gene ATF3 is a target of c-myc in serum-induced cell proliferation. *EMBO J*. 2005;24:2590–2601.
23. Shulman GI. Cellular mechanisms of insulin resistance. *J Clin Invest*. 2000;106:171–176.
24. Haversen L, Danielsson KN, Fogelstrand L, Wiklund O. Induction of proinflammatory cytokines by long-chain saturated fatty acids in human macrophages. *Atherosclerosis*. 2009;202:382–393.
25. Gilchrist M, Thorsson V, Li B, Rust AG, Korb M, Roach JC, Kennedy K, Hai T, Bolouri H, Aderem A. Systems biology approaches identify ATF3 as a negative regulator of Toll-like receptor 4. *Nature*. 2006;441:173–178.
26. Kim HB, Kong M, Kim TM, Suh YH, Kim WH, Lim JH, Song JH, Jung MH. NFATc4 and ATF3 negatively regulate adiponectin gene expression in 3T3–L1 adipocytes. *Diabetes*. 2006;55:1342–1352.
27. Inouye S, Fujimoto M, Nakamura T, Takaki E, Hayashida N, Hai T, Nakai A. Heat shock transcription factor 1 opens chromatin structure of interleukin-6 promoter to facilitate binding of an activator or a repressor. *J Biol Chem*. 2007;282:33210–33217.
28. Akira S, Takeda K. Toll-like receptor signalling. *Nat Rev Immunol*. 2004;4:499–511.
29. Lim JH, Lee JI, Suh YH, Kim W, Song JH, Jung MH. Mitochondrial dysfunction induces aberrant insulin signalling and glucose utilisation in murine C2C12 myotube cells. *Diabetologia*. 2006;49:1924–1936.
30. Lu D, Chen J, Hai T. The regulation of ATF3 gene expression by mitogen-activated protein kinases. *Biochem J*. 2007;401:559–567.
31. Imai Y, Kuba K, Neely GG, Yaghubian-Malhami R, Perkmann T, van Loo G, Ermolaeva M, Veldhuizen R, Leung YH, Wang H, Liu H, Sun Y, Pasparakis M, Kopf M, Mech C, Bavari S, Peiris JS, Slutsky AS, Akira S, Hultqvist M, Holmdahl R, Nicholls J, Jiang C, Binder CJ, Penninger JM. Identification of oxidative stress and Toll-like receptor 4 signaling as a key pathway of acute lung injury. *Cell*. 2008;133:235–249.
32. Horvai A, Palinski W, Wu H, Moulton KS, Kalla K, Glass CK. Scavenger receptor A gene regulatory elements target gene expression to macrophages and to foam cells of atherosclerotic lesions. *Proc Natl Acad Sci U S A*. 1995;92:5391–5395.

Expanded Materials and Methods

Materials and Antibodies

NF-κB inhibitor BAY11-7085, p38 MAPK inhibitor SB203580, and JNK inhibitor SP600125 were purchased from Merck (San Diego, CA). MEK inhibitor U0126 was purchased from Cell Signaling Technology (Danvers, MA). The pEF-p50-NHA and pEF-p60 plasmids which express p50 and p65 subunits of NF-κB, respectively, and the pMRX-SR-IκBα plasmid which expresses a super-repressor form of IκBα (SR-IκBα; a degradation- resistant mutant of IκBα) are described elsewhere.[1,2] LPS (from Escherichia. coli O111: B4) and anti-α-tubulin antibody were purchased from Sigma (San Diego, CA). Palmitate, stearate, and oleate were purchased from Sigma, solubilized in ethanol, and conjugated with fatty acids- and immunoglobulin-free bovine serum albumin (Sigma) at a molar ratio of 10: 1 (fatty acid: albumin) in low serum medium as previously described.[3] The concentrations of palmitate used in this study (< 200 μmol/l) are within the physiologic levels. Antibody against ATF3 was purchased from Santa Cruz (sc-188, Santa Cruz, CA). All other reagents were purchased from Sigma or Nacalai Tesque (Kyoto, Japan) unless otherwise described.

cDNA Microarray Analysis

Serum starved RAW264 macrophages were treated with palmitate (200 μmol/l) or vehicle for 5 h. The epididymal adipose tissue was prepared from 12-week-old male *ob/ob* and wild-type mice. DNA microarray analysis was performed as previously described.[4] In brief, total RNA was extracted using TRIzol reagent (Invitrogen, Carlsbad, CA) and repurified with an RNeasy purification kit (Qiagen, Hilden, Germany). Ten μg of RNA was applied for microarray analysis (Mouse Genome 430A 2.0; Affymetrix, Santa Clara, CA) and GeneChip software (Affymetrix) was utilized for analysis of microarray data.

Co-culture of Adipocytes and Macrophages

Co-culture of adipocytes and macrophages was performed as described.[3,4] In brief, serum starved differentiated 3T3-L1 adipocytes (~0.5 x 10^6 cells) were cultured in a 35-mm dish and macrophages (1.0×10^5 cells of RAW264 macrophages or peritoneal macrophages) were plated onto 3T3-L1 adipocytes. The cells were cultured for 24 h with contact each other and harvested. As a control, adipocytes and macrophages, the numbers of which were equal to those in the co-culture, were cultured separately and mixed after harvest.

Animals

Six-week-old male C3H/HeJ mice which have defective LPS signaling due to a missense mutation in the TLR4 gene[5] and control C3H/HeN mice were purchased from CLEA Japan (Tokyo, Japan). Genetically obese *ob/ob*, *db/db*, and KK*A*^{y} mice were purchased from CLEA Japan and Charles River Japan (Tokyo, Japan). The animals were housed in individual cages in a temperature-, humidity-, and light-controlled room (12-h light and 12-h dark cycle) and allowed free access to water and standard chow (Oriental MF; 362 kcal/100 g, 5.4% energy as fat) (Oriental Yeast, Tokyo, Japan), when otherwise noted. In the high-fat feeding experiments, male mice at 10 weeks of age were given free access to water and either the standard chow or high-fat diet (D12492; 556 kcal/100g, 60% energy as fat; Research Diets, New Brunswick, NJ) for 4 weeks.[6] At the end of the experiments, mice were sacrificed after a 1-h fast under intraperitoneal pentobarbital anesthesia (30 mg/kg). All animal experiments were conducted in accordance to the guidelines of Tokyo Medical and Dental University Committee on Animal Research (No. 0090058).

Generation of Transgenic Mice Overexpressing ATF3 in Macrophages

The 4.96-kb enhancer/promoter of the human scavenger receptor-A (SR-A) gene capable of macrophage-specific expression was kindly provided by Dr. Christopher K. Glass (University of California, San Diego, CA).[7] A full-length human ATF3 cDNA was fused with SR-A enhancer/promoter and a human growth hormone polyadenylation site. The transgene (Online Figure Va) was linearized and microinjected into the pronuclei of C57BL/6J mouse fertilized eggs. To identify founder mouse lines that carried the SR-A enhancer/promoter-ATF3 transgene, Southern blot analysis was performed using tail tissue DNA. Expression of ATF3 mRNA and protein in peritoneal and bone marrow-derived macrophages was evaluated by real-time PCR and Western blotting, respectively.

Chromatin Immunoprecipitation (ChIP) Assay

To assess ATF3 binding to the TNFα promoter, ChIP assay was performed using the ChIP assay kit (Upstate Biotechnology, CA) according to the manufacture's instruction[8]. After stimulation with LPS, cells were fixed in 1% formaldehyde for 15 min at 37°C to cross-link DNA and proteins, lysed, and sheared with a handy sonicator (Tomy Seiko, Tokyo, Japan) to generate DNA ranging in size from 200 to 1000 bp. The lysates were pre-cleared with protein A-agarose and immunoprecipitated by incubating overnight at 4°C with anti-ATF3 antibody (Sant Cruz) or normal rabbit IgG as a negative control. Before immunoprecipitation, "input" samples were removed from the lysates. After immunoprecipitation, protein-DNA complexes were eluted in a buffer containing 1% SDS and 0.1 M $NaHCO_3$, and the cross-links were reversed. The resulting DNA was purified by phenol/chloroform extraction and ethanol precipitation, and subjected to semiquantitative PCR analysis.

The primers used for PCR were designed to amplify the proximal sequence of the mouse TNFα promoter containing the AP-1 site at -926 bp relative to the transcription start site (NM_013693): forward (5'-CAGAGACATGGTGGATTCACG-3') and reverse (5'-GCCCTGCTTCCAGGATTTCTC -3').

Retrovirus-mediated Overexpression and Knockdown of ATF3 in Macrophages

A full-length mouse ATF3 cDNA, consisting of 543 bp encoding 181 amino acid residues, was amplified by PCR with a pair of primers, one with a BamHI site and the other with an EcoRI site at the terminus. The PCR product was inserted into the BamHI/EcoRI cloning sites of the pMRX retroviral vector.[9] The retroviral expression vector (pMRX-mATF3) capable of expressing mouse ATF3 ORF was transfected into Plat-E packaging cells[9, 10] and the retrovirus was harvested 48 h to 72 h after transfection.[11] RAW264 cells were infected with the viral supernatant for 4 h and then cultured in medium supplemented with 10% fetal bovine serum before selection. Puromycin (5 μg/ml) was added to the medium 2 days after the initial infection and the selection was continued for 2 weeks. Stable ATF3-RAW264 cell line was obtained after evaluating the expression levels of ATF3 protein by Western blotting.

pSINsi-hU6 DNA (Code 3661, Takara Bio, Otsu, Japan) for the synthesis of siRNA under the control of the human U6 promoter was used to generate pshATF3 plasmids expressing hairpin RNAs of ATF3 target sequences. The resulting pshATF3#1 and pshATF3#3, synthesizing sequences corresponding to nt 745-763 (5'-GGAACCTCTTTATCCAACA-3') and nt 989-1007 (5'-GCATCCTTTGTCTCACCAA-3'), respectively, of mouse ATF3 mRNA (NM_007498) were used for knockdown of endogenous ATF3. As a control, pshGFP was constructed in the same way and the sequence used to target the GFP gene was as described elsewhere.[12] Retrovirus preparation and RAW264 cell infection are the same as described above except that the selection is under G418 (400 μg/ml, Invitrogen, Carlsbad, CA). Stable shATF3-Raw264 cell line was verified for the knockdown efficiency by Western blotting.

Transient Transfection and Luciferase Assay

A luciferase reporter assay was performed as previously described[4] using the luciferase reporter constructs for ATF3 and TNFα promoters.[13] The luciferase reporter construct with no cis-acting DNA elements was used as a negative control. In brief, RAW264 macrophages or HEK293 cells were transiently transfected by electroporation (Nucleofector system; Amaxa, Gaithersburg, MD) or lipofectamine 2000 (Invitrogen), with a luciferase reporter vector and pRL-TK vector (Promega, Madison, WI) as an internal control for transfection efficiency. The luciferase activity was determined using the Dual-Luciferase Reporter Assay System (Promega).

References

1. Tomita S, Fujita T, Kirino Y, Suzuki T. PDZ domain-dependent suppression of NF-κB/p65-induced Aβ42 production by a neuron-specific X11-like protein. *J Biol Chem.* 2000;275:13056-13060.
2. Hironaka N, Mochida K, Mori N, Maeda M, Yamamoto N, Yamaoka S. Tax-independent constitutive IκB kinase activation in adult T-cell leukemia cells. *Neoplasia.* 2004;6:266-278.
3. Suganami T, Nishida J, Ogawa Y. A paracrine loop between adipocytes and macrophages aggravates inflammatory changes: role of free fatty acids and tumor necrosis factor α. *Arterioscler Thromb Vasc Biol.* 2005;25:2062-2068.
4. Suganami T, Tanimoto-Koyama K, Nishida J, Itoh M, Yuan X, Mizuarai S, Kotani H, Yamaoka S, Miyake K, Aoe S, Kamei Y, Ogawa Y. Role of the Toll-like receptor 4/NF-κB pathway in saturated fatty acid-induced inflammatory changes in the interaction between adipocytes and macrophages. *Arterioscler Thromb Vasc Biol.* 2007;27:84-91.
5. Poltorak A, He X, Smirnova I, Liu MY, Van Huffel C, Du X, Birdwell D, Alejos E, Silva M, Galanos C, Freudenberg M, Ricciardi-Castagnoli P, Layton B, Beutler B. Defective LPS signaling in C3H/HeJ and C57BL/10ScCr mice: mutations in TLR4 gene. *Science.* 1998;282:2085-2088.
6. Suganami T, Mieda T, Itoh M, Shimoda Y, Kamei Y, Ogawa Y. Attenuation of obesity-induced adipose tissue inflammation in C3H/HeJ mice carrying a Toll-like receptor 4 mutation. *Biochem Biophys Res Commun.* 2007;354:45-49.
7. Horvai A, Palinski W, Wu H, Moulton KS, Kalla K, Glass CK. Scavenger receptor A gene regulatory elements target gene expression to macrophages and to foam cells of atherosclerotic lesions. *Proc Natl Acad Sci U S A.* 1995;92:5391-5395.
8. Kamei Y, Miura S, Suganami T, Akaike F, Kanai S, Sugita S, Katsumata A, Aburatani H, Unterman TG, Ezaki O, Ogawa Y. Regulation of SREBP1c gene expression in skeletal

muscle: role of retinoid X receptor/liver X receptor and forkhead-O1 transcription factor. *Endocrinology.* 2008;149:2293-2305.

9. Saitoh T, Nakayama M, Nakano H, Yagita H, Yamamoto N, Yamaoka S. TWEAK induces NF-κB2 p100 processing and long lasting NF-κB activation. *J Biol Chem.* 2003;278:36005-36012.
10. Morita S, Kojima T, Kitamura T. Plat-E: an efficient and stable system for transient packaging of retroviruses. *Gene Ther.* 2000;7:1063-1066.
11. Ito A, Suganami T, Miyamoto Y, Yoshimasa Y, Takeya M, Kamei Y, Ogawa Y. Role of MAPK phosphatase-1 in the induction of monocyte chemoattractant protein-1 during the course of adipocyte hypertrophy. *J Biol Chem.* 2007;282:25445-25452.
12. Caplen NJ, Parrish S, Imani F, Fire A, Morgan RA. Specific inhibition of gene expression by small double-stranded RNAs in invertebrate and vertebrate systems. *Proc Natl Acad Sci U S A.* 2001;98:9742-9747.
13. Cai Y, Zhang C, Nawa T, Aso T, Tanaka M, Oshiro S, Ichijo H, Kitajima S. Homocysteine-responsive ATF3 gene expression in human vascular endothelial cells: activation of c-Jun NH_2-terminal kinase and promoter response element. *Blood.* 2000;96:2140-2148.

Online Figure Legends

Online Figure I. Identification of ATF3 as a Target Gene of Saturated Fatty Acid in Obese Adipose Tissue. (a) cDNA microarray analysis screening for a target of saturated fatty acid/TLR4 signaling in obese adipose tissue. RAW264 macrophages were treated with either palmitate (200 μmol/l) or vehicle for 5 h. The epididymal adipose tissue was prepared from 12-week-old male *ob/ob* or wild-type mice. (b) Tissue distribution of ATF3 and F4/80 mRNAs in mice. WAT, white adipose tissue. Open and closed bars indicate wild-type mice fed standard diet and *db/db* mice fed high-fat diet, respectively. $*P < 0.01$ vs. wild-type mice fed standard diet. $n = 4$-6.

Online Figure II. Role of the TLR4/NF-κB Signaling in ATF3 mRNA Expression in the Interaction between Adipocytes and Macrophages. (a) ATF3 and TNFα mRNA expression in the co-culture between 3T3-L1 adipocytes and peritoneal macrophages obtained from C3H/HeN mice (HeN) or C3H/HeJ mice (HeJ). ct, control culture; co, co-culture. $*P < 0.05$, $**P < 0.01$ vs. the respective ct; $\#P < 0.05$. $n = 4$. (b) Role of NF-κB in the co-culture-induced ATF3 and TNFα mRNA expression. Co-culture was performed using 3T3-L1 adipocytes and RAW264 macrophages. BAY, BAY11-7085 10 μmol/l. $*P < 0.05$, $**P < 0.01$ vs. Veh/ct; $\#P < 0.05$, $\#\#P < 0.01$. $n = 4$.

Online Figure III. Effect of ATF3 Overexpression on IL-6 and iNOS mRNA Expression *in vitro* and *in vivo*. (a) Effect of ATF3 on the palmitate-induced IL-6 and iNOS mRNA expression in RAW264 macrophages overexpressing ATF3 (ATF3) and control RAW264 macrophages (Mock). (b) IL-6 and iNOS mRNA expression in the adipose tissue from WT:KK, Tg:KK, WT:KKA^y, and Tg:KKA^y mice. Veh, vehicle; Pal, palmitate 200 μmol/l; WT, wild-type; Tg, ATF3 transgenic mice. $**P < 0.01$ vs. Veh/Mock; $\#\#P < 0.01$. $n = 4$.

Online Figure IV. Effect of MAPK Inhibitors on Palmitate- and LPS-induced ATF3 and TNFα mRNA Expression in RAW264 Macrophages. Veh, vehicle; Pal, palmitate

100 μmol/l; LPS, LPS 10 ng/ml; U, U0126 5 μmol/l; SP, SP600125 10 μmol/l; SB, SB203580 10 μmol/l. **$P < 0.01$ vs. Veh/Veh, ##$P < 0.01$. $n = 4$.

Online Figure V. Generation of Transgenic Mice Overexpressing ATF3 in Macrophages. (a) Schematic representation of the mouse SR-A promoter/human ATF3 fusion gene. (b) Western blot analysis of ATF3 protein expression in peritoneal macrophages and bone marrow-derived macrophages obtained from three independent transgenic lines (#2, #25, #35) and wild-type mice.

Online Table I. Primers used in this study.

Genes	Primers
Adiponectin	Fw: 5'-ATGGCAGAGATGGCACTCCT-3'
	Rv: 5'-CCTTCAGCTCCTGTCATTCCA-3'
Arginase 1	Fw: 5'-CTCCAAGCCAAAGTCCTTAGAG-3'
	Rv: 5'-AGGAGCTGTCATTAGGGACATC-3'
ATF3	Fw: 5'-TGCCTGCAGAAAGAGTCAGAGA -3'
	Rv: 5'-AGCTCCTCGATCTGGGCC-3'
CD11c	Fw: 5'-CTGGATAGCCTTTCTTCTGCTG -3'
	Rv: 5'-GCACACTGTGTCCGAACTC-3'
F4/80	Fw: 5'-CTTTGGCTATGGGCTTCCAGTC-3'
	Rv: 5'-GCAAGGAGGACAGAGTTTATCGTG-3'
IL-6	Fw: 5'-ACAACCACGGCCTTCCCTACTT-3'
	Rv: 5'-CACGATTTCCCAGAGAACATGTG-3'
iNOS	Fw: 5'- CCAAGCCCTCACCTACTTCC-3'
	Rv: 5'- CTCTGAGGGCTGACACAAGG-3'
Mannose receptor	Fw: 5'- CGGTGAACCAAATAATTACCAAAAT-3'
	Rv: 5'-GTGGAGCAGGTGTGGGCT-3'
TNFα	Fw: 5'- ACCCTCACACTCAGATCATCTTC-3'
	Rv: 5'- TGGTGGTTTGCTACGACGT-3'
36B4	Fw: 5'-GGCCCTGCACTCTCGCTTTC-3'
	Rv: 5'-TGCCAGGACGCGCTTGT-3'

Online Table II. Up-regulated genes both in obese adipose tissue and saturated fatty acid-stimulated macrophages.

Accession ID	Gene Symbol	Gene Title	Adipose tissue (*ob/ob* vs. WT)	RAW264 (Pal vs. Veh)
NM_031167	Il1rn	interleukin 1 receptor antagonist	15.0	2.6
NM_015811	Rgs1	regulator of G-protein signaling 1	14.8	2.8
NM_010442	Hmox1	heme oxygenase (decycling) 1	8.6	3.5
M57525	Il1rn	interleukin 1 receptor antagonist	8.6	2.1
NM_023044	Slc15a3	solute carrier family 15, member 3	8.6	3.7
BC022752	Slc37a2	solute carrier family 37 (glycerol-3-phosphate transporter), member 2	8.6	2.3
AF065933	Ccl2	chemokine (C-C motif) ligand 2	7.8	3.2
BC019946	Atf3	activating transcription factor 3	5.2	4.3
AV026617	Fos	FBJ osteosarcoma oncogene	5.2	4.3
NM_011315	Saa3	serum amyloid A 3	4.9	2.0
NM_008871	Serpine1	serine (or cysteine) proteinase inhibitor, clade E, member 1	4.7	17.1
BM210600	Npn3	neoplastic progression 3	4.4	2.3
AK011545	Basp1	brain abundant, membrane attached signal protein 1	4.4	2.6
NM_138648	unknown	unknown	4.3	2.1
NM_013612	Slc11a1	solute carrier family 11 (proton-coupled divalent metal ion transporters), member 1	4.1	2.0
BC011325	Npn3	neoplastic progression 3	3.7	2.6
AF128193	Ccl7	chemokine (C-C motif) ligand 7	3.2	3.0
NM_008129	Gclm	glutamate-cysteine ligase , modifier subunit	2.6	2.8
NM_016903	Esd	esterase D/formylglutathione hydrolase	2.4	2.3
M57525	Il1rn	interleukin 1 receptor antagonist	2.3	2.1

ob/ob and WT, 12-week-old male *ob/ob* and wild-type mice, respectively. Pal, palmitate 200 μmol/l; Veh, vehicle.

Online Table III. Down-regulated genes both in obese adipose tissue and saturated fatty acid-stimulated macrophages.

Accession ID	Gene Symbol	Gene Title	Adipose tissue (*ob/ob* vs. WT)	RAW264 (Pal vs. Veh)
NM_026713	Mogat1	monoacylglycerol O-acyltransferase 1	-5.9	-2.0
BB560574	Cd24a	CD24a antigen	-3.9	-3.2
NM_007446	Amy1	amylase 1, salivary	-3.0	-2.5
BI686700	LOC216024	Similar to heterogeneous nuclear ribonucleoprotein H3, isoform a	-2.5	-2.3
BG074158	2610001E17Rik	RIKEN cDNA 2610001E17 gene	-2.4	-2.3

ob/ob and WT, 12-week-old male *ob/ob* and wild-type mice, respectively. Pal, palmitate 200 μmol/l; Veh, vehicle.

Online Table IV. Body weight and adipose tissue weight of C3H/HeJ and C3H/HeN mice on a standard or high-fat diet for 16 weeks.

	body weight (g)	epididymal WAT weight (g)	mesenteric WAT weight (g)
SD-fed HeN	27.1 ± 0.8	0.21 ± 0.03	0.17 ± 0.03
HD-fed HeN	39.3 ± 0.8*	0.54 ± 0.04**	0.47 ± 0.02**
SD-fed HeJ	31.2 ± 1.0	0.31 ± 0.07	0.18 ± 0.05
HD-fed HeJ	41.0 ± 0.8##	0.61 ± 0.03##	0.43 ± 0.03##

SD, standard diet; HD, high-fat diet; HeN, C3H/HeN; HeJ, C3H/HeJ; WAT, white adipose tissue. *$P < 0.05$, **$P < 0.01$ vs. SD-fed HeN, ##$P < 0.01$ vs. SD-fed HeJ, n = 6-10.

a

	RAW264 macrophages palmitate vs. vehicle		Adipose tissue *ob/ob* vs. wild-type
Up-regulated (> 2-fold)	214	20	798
Down-regulated (< 2-fold)	188	5	860

b

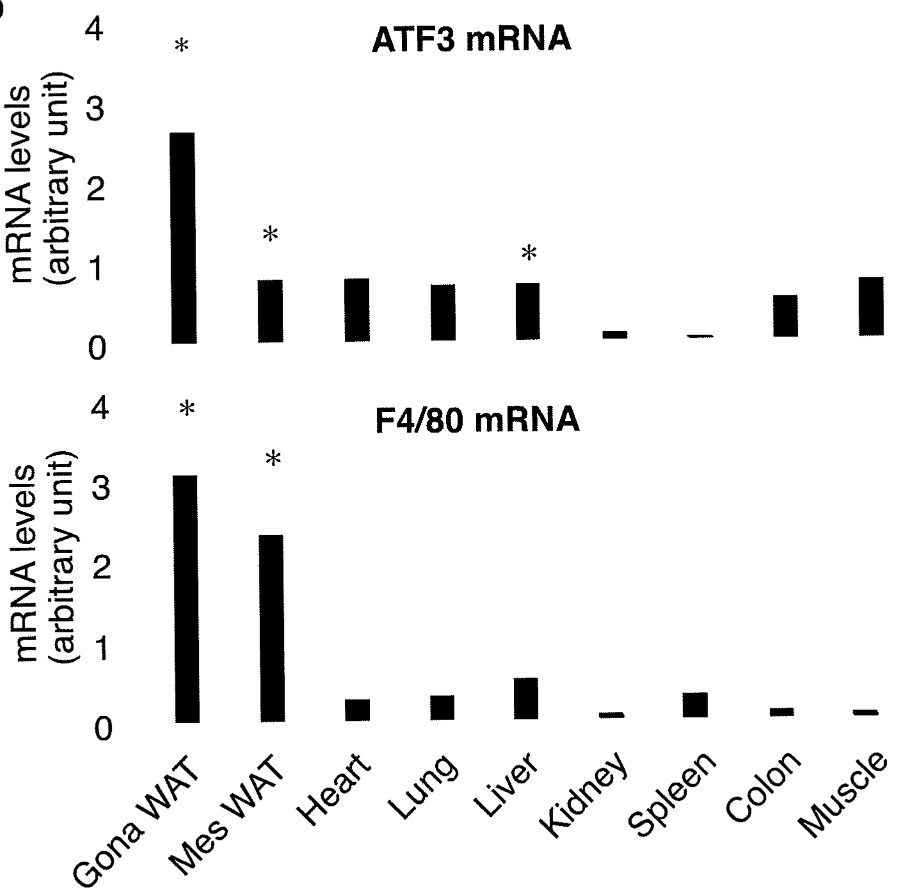

Online Figure I

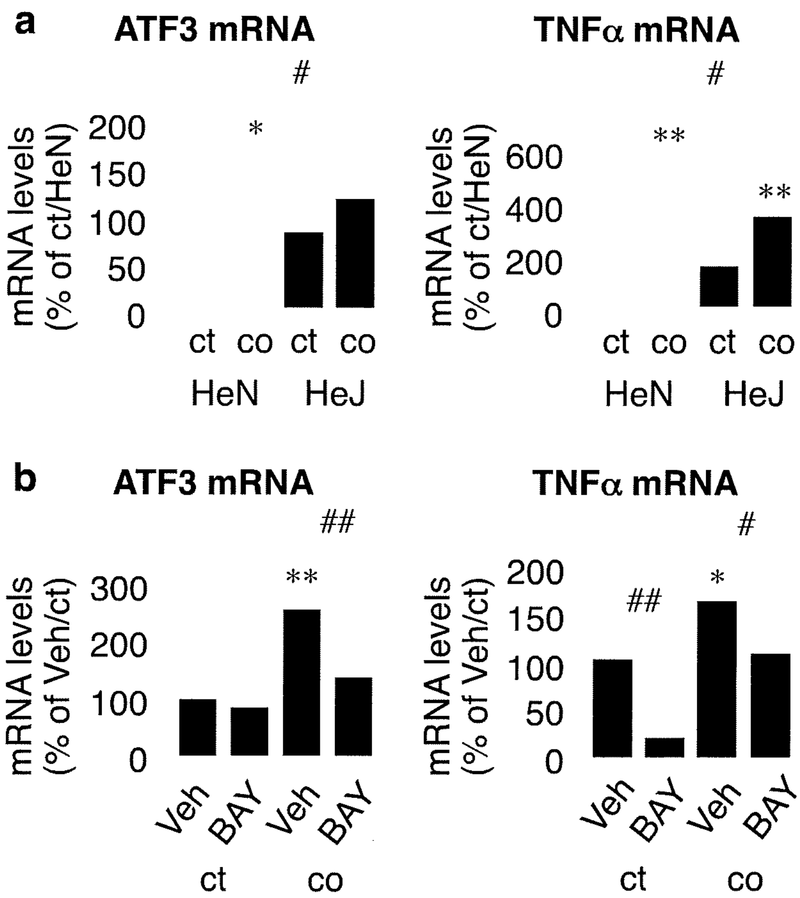

Online Figure II

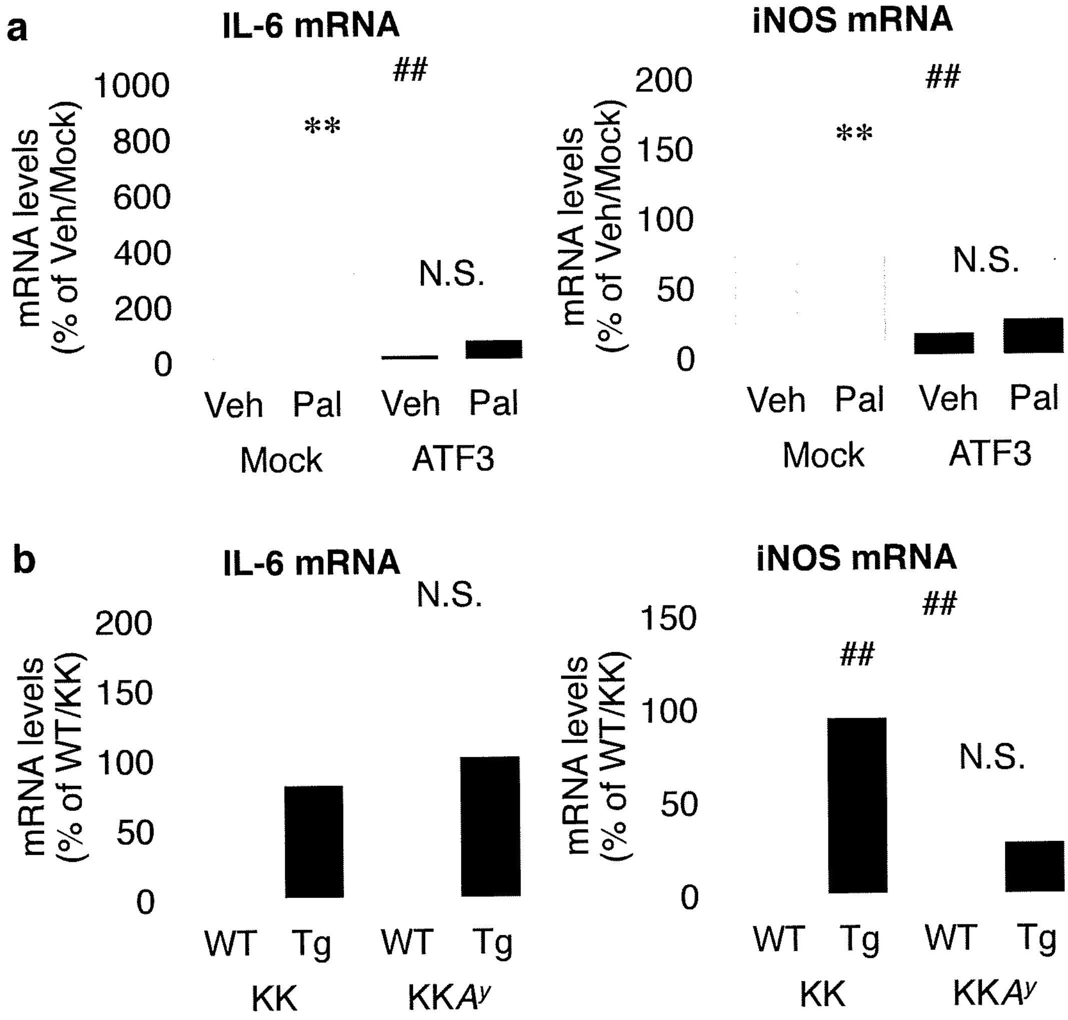

Online Figure III

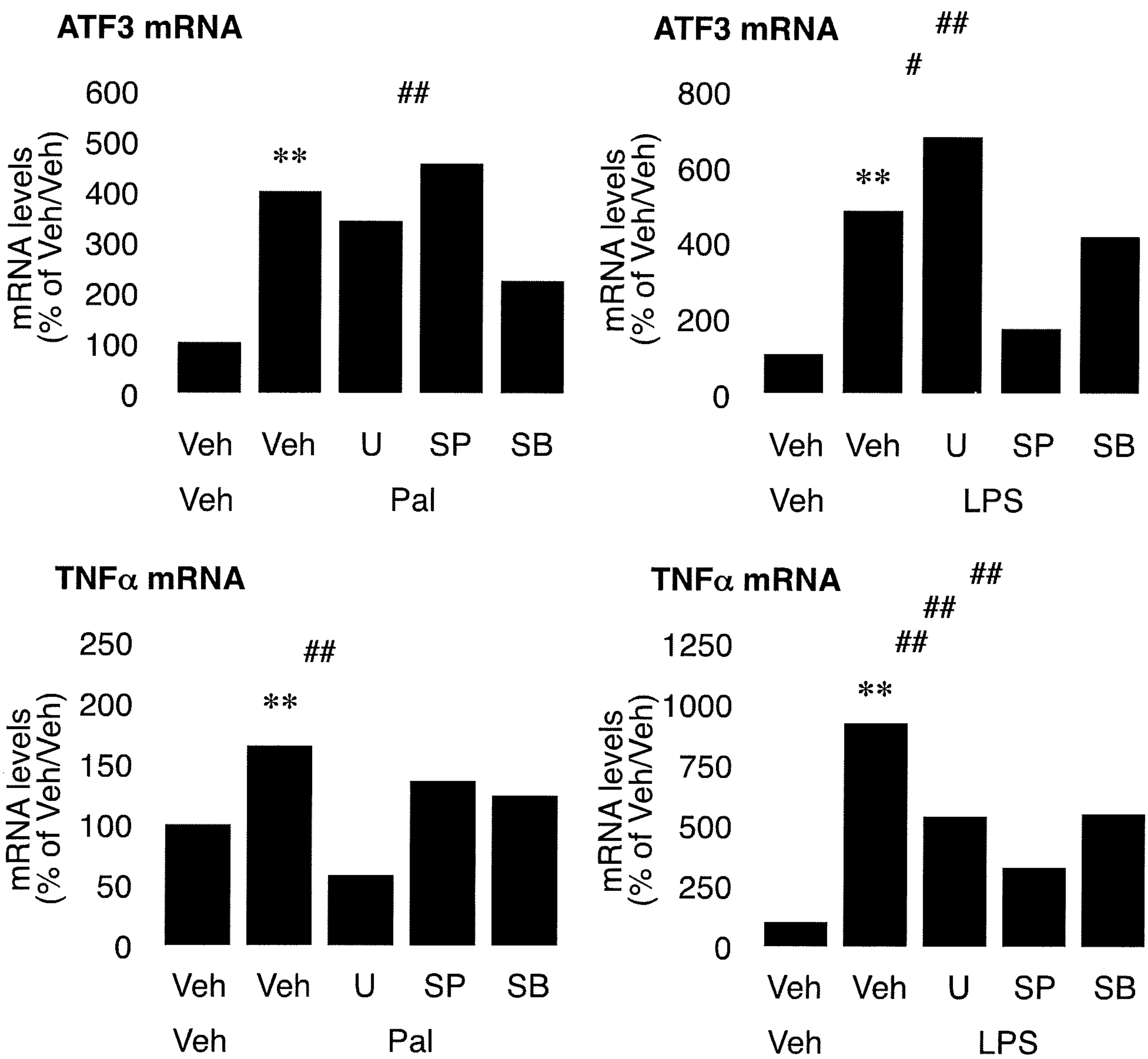

Online Figure IV